OH Formation from O and H Atoms Physisorbed on a Graphitic Surface through the Langmuir−Hinshelwood Mechanism: A Quasi-Classical Approach

H. Bergeron,*,† N. Rougeau,† V. Sidis,‡ M. Sizun,‡ D. Teillet-Billy,‡ and F. Aguillon†

Université Paris-Sud, Laboratoire des Collisions Atomiques et Moléculaires, UMR8625 F-91405, Orsay, France

Received: June 10, 2008; Revised Manuscript Received: August 8, 2008

We study the quasi-classical dynamics of OH formation on a graphitic surface through the Langmuir−Hinshelwood (LH) mechanism when both O and H ground-state atoms are initially physisorbed on the surface. The model proceeds from previous theoretical work on the LH formation of the H_2 molecule on graphite [Morisset, S.; Aguillon, F.; Sizun, M.; Sidis, V. *J. Chem. Phys.* **2004**, *121*, 6493; ibid **2005**, *122*, 194704]. The H-graphite system is first revisited with a view to get a tractable DFT-GGA computational prescription for the determination of atom physisorption onto graphitic surfaces. The DZP-RPBE combination is found to perform well; it is thereafter used along with MP2 calculations to determine the physisorption characteristics of atomic oxygen on graphitic surfaces. We also deal with chemisorption. In accordance with previous work, we find that O chemisorbs on graphite in a singlet spin state epoxy-like conformation. In the triplet state we find only "metastable" chemisorption with an activation barrier of 0.2 eV. The physisorption results are then used in the LH dynamics calculation. We show that in the [0.15 meV, 12 meV] relative collision energy range of the reacting O and H atoms on the surface, the OH molecule is produced with a large amount of internal energy (≃4 eV) and a significant translation energy (≥100 meV) relative to the surface.

I. Introduction

Atomic oxygen (O) is after hydrogen (H) and helium (He) the most abundant element in the interstellar medium (ISM); with an abundance between 5×10^{-4} and 8×10^{-4} relative to H, it is twice as abundant as the next element carbon. Thence O and H atoms may recombine in the ISM to produce OH (the hydroxyl radical). OH is indeed an eminent molecular constituent of the ISM. Its formation there is an important step for the synthesis of a variety of interstellar XOH molecules among which water (H_2O, X = H) is the most abundant representative particularly in molecular clouds where it is essentially in the form of ice covering dust grains.[1] OH formation is thus an important issue for the physics and chemistry of the ISM; in particular it is a crucial step in the reactions leading to the appearance of water and subsequently of life in the universe.[1,2]

Differently from the H−H recombination into H_2, which can barely take place in the gas phase of the ISM via three body association or radiative recombination, OH can be formed in the gas phase, albeit in ionized regions. This involves a succession of three ion−molecule reactions involving a proton transfer[3]

$$O + H_2^+ \text{ (or } H_3^+) \rightarrow OH^+ + H \text{ (or } H_2)$$

$$OH^+ + H_2 \rightarrow H_2O^+ + H$$

$$H_2O^+ + H_2 \rightarrow H_3O^+ + H$$

finally followed by a dissociative recombination reaction

$$H_3O^+ + e^- \rightarrow OH + H_2$$

Yet it is now well acknowledged that, of the possible formation mechanisms of OH in the ISM, the more straightforward heterogeneous catalysis reactions on grains are the most competitive[3]

$$O + H + \text{grain} \rightarrow OH + \text{grain}$$

Thus the above gas phase reactions are only mentioned for completeness.

The ISM dust grains are believed to be composed of carbonaceous or silicaceous material; in molecular clouds the grains are most probably covered by ice mantles. The catalytic reaction leading to OH may proceed according to the Eley−Rideal (ER)[4] or hot atom (HA) mechanisms[5] which involve the interaction between an O atom adsorbed on the grain surface and an H atom from the gas phase (or vice versa). It may also proceed alternatively according to the Langmuir−Hinshelwood (LH) mechanism in which the O and H atoms are both adsorbed on the grain; the atoms migrate on the surface until they meet each other and then recombine.[4]

In the present work we are concerned with carbonaceous dust grains. In these conditions the surface of the grain is usually modeled as a graphite (0001) surface. Given the large interlayer distance in graphite (3.4 Å) one may restrict the surface to its outermost layer: a graphene sheet. It is also quite frequent to have this sheet approximated using a cluster model: a polycyclic aromatic hydrocarbon (PAH) platelet with (or without) the C−C bond distance adjusted to that of graphite. This is a sensible approximation given especially the interrelationship between PAHs, hydrogenated amorphous carbon, protographitic clusters, and carbonaceous grains.[6] A few examples of work that made use of such a cluster model of graphite may be found in articles cited below.

Atom-surface adsorption can be of two types, namely: chemisorption (which involves tight electron sharing or electron

* To whom correspondence should be addressed. E-mail: herve.bergeron@u-psud.fr.

† Université Paris-Sud, Laboratoire des Collisions Atomiques et Moléculaires.

‡ CNRS, Laboratoire des Collisions Atomiques et Moléculaires.

10.1021/jp8050966 CCC: $40.75
Published on Web 10/25/2008

transfer) or physisorption (which involves weak and distant van der Waals VdW interactions).

H atom chemisorption onto a graphite (0001) surface takes place exclusively atop a C atom of the lattice.[7–10] Yet this involves a change of hybridization from sp^2 to sp^3 of the adsorbent atom as well as surface puckering: the adsorbent C atom moves out of the substrate plane toward the approaching H. It is now well established that this leads to the existence of an activation barrier against H chemisorption of ≈0.2 eV.[7–11] Thus for temperatures below ≈2000 K H atoms interact with a graphitic surface exclusively via physisorption type interactions.

O atom chemisorption onto a graphite (0001) surface takes place preferentially in an electronic singlet spin state:[12–16] the most stable chemisorption site is the bridge site above a C−C bond (epoxy-like structure with a three member C−O−C ring); another, albeit less stable chemisorption site is atop a C atom. But in ISM clouds, O atoms are most likely to be found in their ground ^{3}P state (noted ^{3}O throughout); therefore when a ^{3}O atom adsorbs on the graphite singlet state surface it forms a triplet state. Literature on the spin triplet O-graphite chemisorption is rather scarce. Periodic DFT (density functional theory) calculations of ref 14 using the PW91[18] GGA (generalized gradient approximation) functional, and taking substrate relaxation (puckering) into account, gave a triplet O-graphite chemisorption binding energy of 0.34 eV at the bridge site (this is 1.6 eV above the singlet most stable state). Subsequent ONIOM[19,20] calculations at the bridge site[15] using the B3LYP[21–23] hybrid functional yielded a triplet O-graphite chemisorption binding energy on the planar unrelaxed substrate of 0.93 eV (0.2 eV above the singlet). Anyway, knowledge of the chemisorption binding energy alone is insufficient to characterize the O-graphite adsorption. What is actually needed is the potential energy curve along the minimum energy path for the ^{3}O-graphite adsorption and especially information on an eventual activation barrier. In this respect Goumans et al.[24] asserted, on the basis of DFT MPWB1K[25] calculations on coronene ($C_{24}H_{12}$), that for temperatures below 10 000 K the interaction of a ^{3}O atom with a carbonaceous surface would be governed solely by the physisorption potential. Anticipating on the account of the present results, let us mention in this place our finding of activation barriers of 0.5−0.2 and 0.18 eV for ^{3}O chemisorption on a graphitic-type surface at the bridge and top positions, respectively.

In the temperature conditions of the ISM (few tens of K), the existence of activation barriers against chemisorption of H and ^{3}O atoms on graphitic surfaces preclude the latter adsorption mode. Would this not be the case, one would then have to care about the existence or not of activation barriers for the ER and LH mechanisms of interest when those involve chemisorbed H and ^{3}O atoms. As an indication, typical values of activation barriers for the ER and LH reactions for a singlet chemisorbed O atom are 0.15−0.29 and 1.43 eV, respectively.[16,17] Again these figures are exceedingly large for the cold ISM.

In the present study, we thus consider the LH associative desorption reaction between H and ^{3} O atoms both physisorbed on a graphitic surface. While the physisorption characteristics of H onto graphite are known from both experiment[28] and MP2 (Möller Plesset 2nd order perturbation theory) quantum chemistry calculations[29] those of ^{3}O are not. In astrophysical models for ice formation and growth on grains, estimates of unknown physisorption binding energies are often deduced, using a proportionality rule, from known data on polarizabilities of the considered species.[3,30] The estimate for O on graphite is taken between 45 meV (close to the physisorption energy of H) and 67 meV.[1,30] In a study of OH and H_2O formations on models of amorphous hydrogenated carbon grains, Papoular[31] performed semi empirical AM1 (Austin model 1) calculations to obtain physisorption binding energies for O, OH, and H_2O on typical hydrocarbon functional groups. For O he found adsorption sites with binding energy of 26 meV. This is surprisingly too low. Whatever AM1 is suitable or not to evaluate physisorption energies, let us just mention at this point that the corresponding adsorption site lies along the functional CH group (at 2.2 Å from the H atom) and not above aromatic rings of graphitic surfaces as those considered here. Thus, prior to the LH dynamics calculations we have endeavored to better ascertain the physisorption binding energy of ^{3}O to a graphitic surface. This has been done using a combination of DFT-GGA and MP2 calculations. Meanwhile, in a study of the ^{3}O + CO addition reaction on a carbonaceous surface, Goumans et al.,[24] determined from 6-311G* DFT MPWB1K[25] calculations on coronene, the value of 70.7 meV for the physisorption binding energy of ^{3}O at the preferred bridged position.

In previous works, we have investigated theoretically the quantum and classical dynamics of the LH reaction for the H−H recombination of physisorbed and mobile H atoms on a model graphitic surface representing a carbonaceous dust grain.[26,27] Here we extend these studies to the case of the O−H recombination. This is achieved following the pattern of refs 26 and 27: the physisorbed ^{3} O and H atoms interact via pair wise potentials and move toward each other on a flat and rigid graphitic surface i.e. without any energy accommodation to the surface. Following refs 26 and 27 the recombination process occurs as a result of momentum transfer in the atom-atom collision and scattering near the surface. The collision causes one atom to be sent toward the vacuum and the other atom toward the surface; the latter atom thus rebounds and finally moves toward the vacuum too. This gives rise to a quite stretched molecule that contains substantial vibrational and rotational energy. In the simplest case, the translational energy of the nascent molecule is large enough to lead to a direct desorption; this is the so-called direct mechanism. Otherwise, the molecule is trapped in a quasi stationary state where it oscillates in the physisorption well with a significant amount of vibrational and rotational energy. As these molecular motions are hindered by the surface there is a coupling between them and the molecule translation relative to the surface which allows for the escape of the molecule; this is the so-called complex mechanism.

In as much as quasi classical trajectory (QCT) calculations successfully reproduced the salient features of the quantum LH dynamics results for the H−H recombination[26,27] we have found it expedient to use QCT calculations in the present work. This approximation is expected to work even better for O−H than it does for H−H owing to the substitution of a light atom by a much heavier one.

From this point onward we will use O for ^{3}O except if stated otherwise.

The outline of the paper is as follows. In section II we determine the H-Gr, O-Gr, and O−H interaction potentials involved in our LH recombination model (Gr stands for graphitic grain surface). In section III we present the equations and the procedure underlying the QCT dynamics calculations. The results are analyzed and discussed in sections III.C and III.D. Conclusions are drawn in section IV.

II. Interaction Potentials

A. Computations. As recalled in the Introduction, the carbonaceous grain is represented as a single layer of graphite

(0001): a graphene sheet. The latter surface is suitably modeled using PAH molecules.[7,8,10,15,17,24,29,32,33]

1. H-Gr Physisorption. As mentioned in Sec. I the H-graphite physisorption energy is known from experiment[28] to amount to: 43.3 (±0.5) meV.

Previous DFT calculations using the PW91[18] GGA functional[7–9] were unsuccessful in reproducing these figures. It is well-known that DFT at the mere LDA (local density approximation) or LSD (local spin density) levels dramatically overestimates the binding in the VdW tail of the interaction potentials (see e.g. ref 7). The inclusion of the GGA correction results in a strong reduction of this binding. For the H-graphite physisorption, periodic calculations using plane waves[9] and cluster calculations on coronene ($C_{24}H_{12}$) using a TZP (triple-ζ + polarization) basis set expansion[8] yielded nearly the same result: 8 meV at an H-graphite distance of ≃4.2 Å. Cluster calculations on coronene using a DZP (double-ζ + polarization) basis set expansion[7] yielded a deeper well: between 67 and 74 meV (depending on the physisorption site) at an H-graphite distance of 2.6−2.8 Å. The difference between the two sets of DFT calculations was unambiguously attributed to BSSE (basis set superposition error).

Bonfanti et al.[29] resorted to MP2 calculations and found physisorption binding energies in the range between 34 and 40 meV at distances close to 3 Å in much better agreement with experiment.[28] The binding energies are very little site dependent and calculations show[29] that hydrogen atoms physisorbed on graphite are highly mobile on the surface even at a temperature of 0 K.

MP2 calculations are far less manageable than DFT ones for atom adsorption on large aromatic systems (see below). Therefore we have endeavored to get in the DFT-GGA framework a tractable and trustworthy procedure that could next be used in the determination of O-graphite physisorption characteristics. The sought procedure is first assessed on the H-graphite physisorption. Currently used GGAs have an intrinsic error that causes the physisorption potential well to be too shallow. We have thereby surmised that this error can be favorably canceled by the BSSE of DZP basis sets and have undergone to examine this proposal.

Our DFT-GGA calculations are based on the unrestricted Kohn−Sham approach and make use of the ADF 2007 code.[36] The basis sets of Slater-type orbitals provided with the ADF package are used. As in previous work,[7,8,32] the calculations are carried out with PAH molecules, whose C−C and C−H bond lengths are set fixed to 1.415 Å (as in graphite) and 1.09 Å, respectively. The atom adsorption is studied at three sites along a line perpendicular to the surface plane: atop a carbon atom (*A*), above the middle of a C−C bond (bridge site *B*), and above the hollow site at the center of a carbon ring (*H*). For the *H* physisorption case we have examined benzene (C_6H_6), pyrene ($C_{16}H_{10}$), coronene ($C_{24}H_{12}$), circumpyrene ($C_{42}H_{16}$), and circumcoronene ($C_{54}H_{18}$).

Figure 1 shows the H-coronene physisorption characteristics at the hollow site of the central carbon ring as computed from DFT calculations using three different GGAs, namely: PW91,[18] RPBE,[34,35] and BLYP,[21,22] with the same ADF DZP basis. The results are compared with the MP2 result of ref 29. Of the three DFT results, the RPBE-DZP combination is seen to perform best. The PW91-DZP result is too attractive whereas the BLYP-DZP one, although possibly acceptable in the well region, is marred by its asymptotic behavior. We thus retained the prescription of using the RPBE-DZP combination.

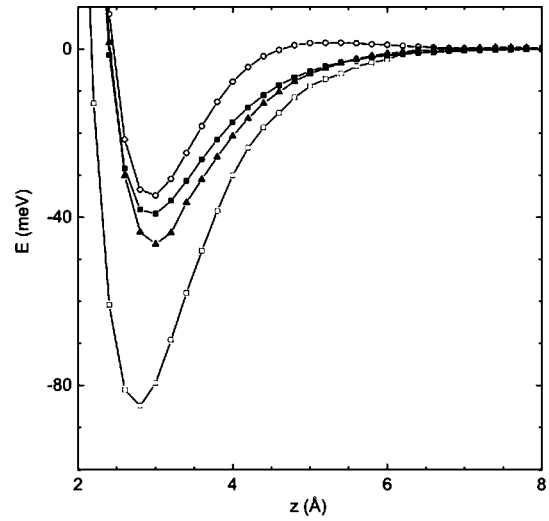

Figure 1. H-coronene physisorption energies as functions of H-coronene distance; Hollow site. PWP91-DZP (open squares), RPBE-DZP (closed triangles), MP2 ref 29 (closed squares) and BLYP-DZP (open circles).

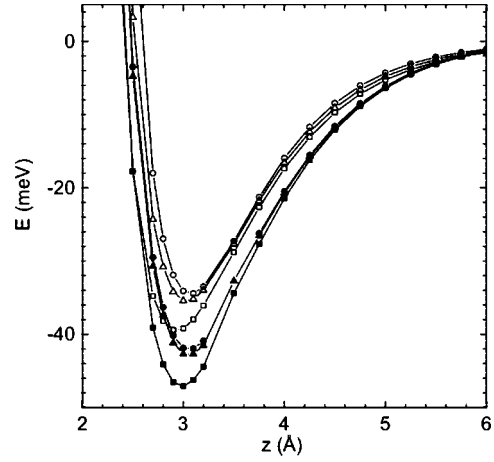

Figure 2. H-coronene physisorption energies as functions of H-coronene distance. Hollow site: squares, Top Site: triangles, Bridge site: circles; RPBE-DZP: closed symbols; MP2 ref 29: open symbols.

The H-coronene physisorption characteristics at the different sites closest to the center of the graphitic platelet evolve with the cluster size. For the hollow site (*H*), the properties are converged at the coronene size. For the bridge site (*B*), the properties are nearly converged at the pyrene size, and for the on top site (*A*), they are already converged at the pyrene size.

Figure 2 shows a comparison of the site dependences of the present RPBE-DZP calculations with the MP2 results of ref 29. Though the former potentials are on the whole slightly deeper than the latter ones, the comparison is quite satisfactory especially in view of the agreement with the experimental data[28] (see Figure 6 below).

2. O-Gr Physisorption. In this section we endeavor to determine the adsorption characteristics of a ^3O atom on a graphitic surface with a special focus on physisorption. The Gr surface is represented by a PAH as indicated in the preceding section. The calculations make use of the above proposed RPBE-DZP prescription and, wherever possible, MP2 calculations. In all these calculations and until we address chemisorption (section IIA3) the atom positions of the graphitic substrate do not relax.

The MP2 calculations have been carried out using the GAMESS[37] computer code. The aug-cc-pVDZ (augmented

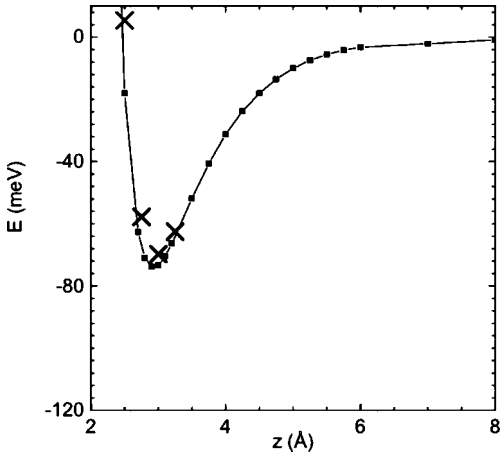

Figure 3. O-benzene physisorption energies as functions of O-benzene distance; Hollow site. RPBE-DZP (closed squares), MP2-ADZ (crosses).

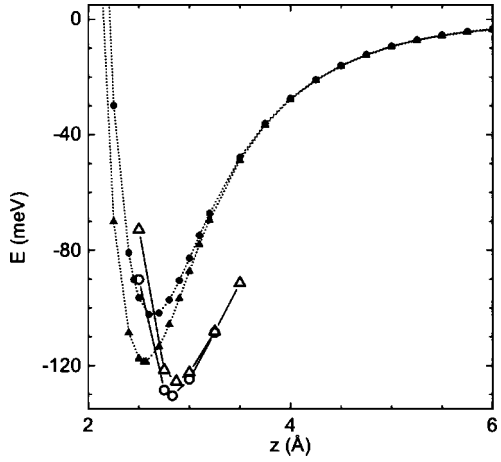

Figure 4. O-pyrene physisorption energies as functions of O-pyrene distance. Bridge site: triangles, Top site: circles; RPBE-DZP: closed symbols; MP2: open symbols.

correlation consistent polarized valence double- ζ) basis set, provided with this code, was used for each atom in the O-PAH system. For the 0th order step of the calculations, the UHF (unrestricted Hartree−Fock) self-consistent field scheme was used. This step is particularly awkward to achieve. Indeed, aside from quasi linear dependence problems with the basis, the convergence is quite capricious and time-consuming. Because of these problems the MP2 calculations could hardly be extended beyond the O-pyrene case. Following the detailed work of Makarewicz[38] on argon-benzene and argon-fluorobenzene VdW complexes we have taken it for granted that the error resulting from incompleteness of aug-cc-pVDZ basis sets is almost exactly canceled by the correlation error inherent in the MP2 method. Therefore, our MP2 results are not corrected for BSSE; following ref 38 they are referred to as MP2-ADZ throughout.

Figure 3 shows results for O physisorption above the hollow site of benzene. These results nicely confirm the procedure prescribed in section IIA1: the RPBE-DZP curve is the one agreeing best with our MP2-ADZ results. The physisorption well in this case has a depth of $\simeq$70 meV and is located at a distance of 3 Å.

Figure 4 shows O-pyrene physisorption results for the on top site and the bridge site.

For pyrene the hollow site may sit along an axis containing (||), or perpendicular to ($\perp$), the central C−C bond. For the hollow site we find, consistently with Figure 4, that the minimum of the potential well lies at 2.9 Å and amounts to 114 meV in the RPBE-DZP (|| and $\perp$ cases) and respectively 2.83 Å and 113 meV in the MP2-ADZ *H* (|| case).

RPBE-DZP calculations around the ground-state potential minimum could also be carried out on the larger O-coronene case for the A and B sites. They confirm the above-reported results which have thereafter been used in the dynamics calculations. For the hollow case and larger PAHs, multiple difficulties have arisen that make the results unreliable.

To see how these results depend on the basis set size and to have an estimate of the BSSE, we have carried out RPBE-TZP calculations for the O-pyrene and O-coronene systems at the bridge and top sites. Surprisingly enough the DZP and TZP physisorption binding energies for both systems at the top site differ by only 2 meV. Differences at the bridge site are of 6 meV for coronene and 16 meV for pyrene. In this latter case the shallower TZP potential minimum moves outward by 0.1 Å. These tests strengthen our confidence in the above-reported results. Compared with the TZP(6-311G*) DFT MPWB1K results of Goumans et al.[24] for the bridged position on coronene our RPBE physisorption binding energy is larger by 50 meV. However, both our results and those of Goumans et al. indicate that O physisorption onto the basal plane of graphitic surfaces is stronger for O than its is for H.

In our results, excluding benzene, the values of the O-Gr physisorption potential minima are seen to be larger than the H-Gr one by a factor of $\simeq$3. This result is unexpected on the basis of the proportionality of VdW potentials to the polarizabilities of the involved species; thus it is quite plausible that it involves some electron transfer from the substrate to the atom. Charge analyzes (Mulliken, Hirschfeld, Voronoi) of the RPBE DZP and TZP results at the potential minimum indeed indicate a slight negative charge (−0.07 to −0.1) on the O atom. The UHF-ADZ results also show comparable Mulliken charges. However the UHF-ADZ potential curves are always repulsive. The well appears only at the (post UHF) MP2 stage. This indicates that the invoked charge transfer is an effect of electron correlation. For comparison and in support of the above explanation we point out that the charge transfer in the H-Gr system is an order of magnitude smaller in the physisorption well region.

3. O-Gr Chemisorption. The above calculations for the ^{3}O adsorption on the unrelaxed platelet show no indication of chemisorption except a slight shoulder in the repulsive wall of the interaction potential for the bridge site around 1.6 Å. This is already at variance with the ONIOM-B3LYP unrelaxed results of ref 15 which predict triplet chemisorption with a binding energy of 0.93 eV (0.2 eV above the singlet).

We have next carried out RPBE-DZP calculations on both the singlet and triplet adsorption at the bridge and top sites with relaxation allowed. In these calculation the two C atoms beneath the approaching O atom in the bridge position and the C adsorbent atom in the top position may relax.

For the singlet case we find in accordance with previous work[12−16] that the bridge site provides the strongest chemisorption binding energy; this chemisorption position is found to lie at a distance z_{chem} = 1.5 Å of the O atom above the basal plane of the platelet. The calculated binding energy, relative to the ^{3}O + Gr asymptotic level limit, amounts to 2.7 eV for pyrene and 2.6 eV for coronene. In agreement with previous work,[12,13] we also find another chemisorption site atop a C carbon of the lattice. At the top site the binding energy is of 1.64 eV for pyrene and 1.7 eV for coronene at a distance z_{chem} = 1.8 Å. Our results for the bridge site are

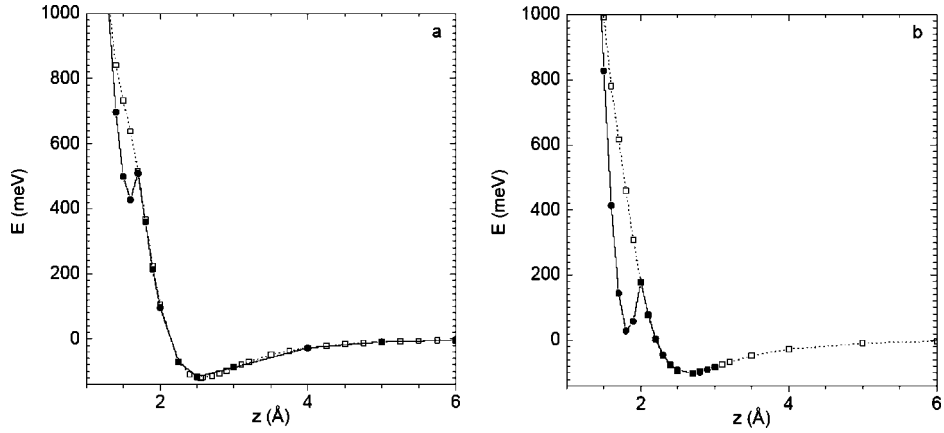

Figure 5. Profile of the triplet spin O-pyrene interaction potential along the minimum energy path as a function the distance of the O atom to the basal plane. Results with surface relaxation allowed (full line and closed symbols) are compared with those obtained for the flat unrelaxed surface (dotted line and open symbols): (a) bridge site and (b) top site.

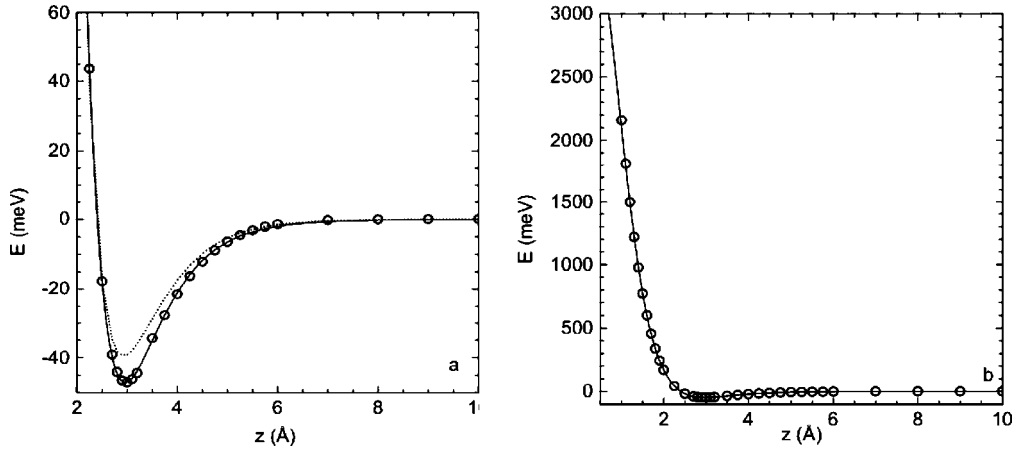

Figure 6. (a) H-coronene physisorption energies as functions of H-coronene distance; Hollow site. RPBE-DZP (closed circles), Fit of eq 1 (full line), MP2-ADZ of ref 29 (dotted line). (b) Same as Figure 6a for the complete z-range.

in good agreement with the periodic PBE calculations of Jelea et al.[16] (2.5 eV). Reasonable accord is also found with the relaxed periodic PW91 calculations of Incze et al.[13] (3.02 eV). A somewhat greater difference is found with the result of Sorescu et al.[14] periodic PW91 calculations (1.9 eV). Yet we find it quite astonishing that the latter two calculations[13,14] that employed the same functional and the same computer code yield so different results. ONIOM-B3LYP unrelaxed calculations[15] yielded a binding energy of only 1.13 eV. Relaxed DFT B3LYP calculations[15] on the ($C_{42}H_{16}$) PAH yielded a still lower value: 0.9 eV. Putting aside the latter three discrepant results and considering that our singlet chemisorption energy is validated by the comparisons with refs 13 and 16, we may turn next to the triplet case.

Let us mention right away that no real chemisorption is found in the present RPBE-DZP results for the triplet state. One should first note that for atom−substrate distances $z >$ 2 Å the ^{3}O−Gr interaction potential is not affected by the relaxation freedom given to the system. As shown in Figure 5 a cusp appears at ≃1.8 Å for the bridge site and 2 Å for the top site on the repulsive wall of the physisorption potential; this is then followed by a well that hangs above the ^{3}O + Gr asymptotic level. This depicts a "metastable chemisorption" situation. The apex of the cusp determines the height of the activation barrier for the latter ^{3}O "metastable chemisorption". For pyrene and coronene the barrier height at the bridge site is of 0.5 and 0.2 eV, respectively. For the pyrene top site it is of 0.15 eV. The only other calculations on triplet chemisorption are as indicated in Sec. I those of refs 14 and 15. In as much as these works were already put aside for their discrepancies in the singlet chemisorption case and since they are not in better mutual agreement for the triplet case either, we do not consider them any further. Therefore, based on the internal consistency of our calculations and on their validation as discussed above for the singlet chemisorption and triplet physisorption, in the following we rely on our triplet state results. Thus owing to the aforementioned barriers against chemisorption this latter adsorption mode is not operative in the temperature conditions of the ISM clouds. Accordingly, in the forthcoming sections only the ^{3}O−Gr physisorption characteristics obtained above (section IIA2) are retained.

B. Fitting Formula for the H-Gr and O-Gr Physisorption Potentials. Previous studies of the H−H recombination via the LH mechanism[26,27] used a potential form proposed by Ghio et al.[28] In the present work we have introduced and used a modified version of the Ghio potential.

Our potential contains two terms: a repulsive term (a sigmoid) that represents the repulsive effect of the electrons of the surface and an attractive term that represents the dipole−dipole interactions.

$$V_{\mathrm{Atom-Gr}}(z) = K\left[\frac{a}{1+\mathrm{e}^{\alpha(z-z_0)}} - \frac{1}{[1+(\alpha(z-z_1))^2]^n}\right] \quad (1)$$

z is the distance of the atom from the surface plane; K, α, β, z_0, z_1, and n are fitting parameters and do not have any particular

TABLE 1: Parameters of the V_{Gr-H} Potential

K (meV)	a	α (Å^{-1})	z_0 (Å)	β (Å^{-1})	z_1 (Å)	n
2326.88	2.02075	2.53937	1.73772	0.657003	1.35938	3.0

TABLE 2: Parameters of the V_{Gr-O} Potentials (B: Bridge, A: Atop, and H: Hollow)

	K (meV)	a	α (Å^{-1})	z_0 (Å)	β (Å^{-1})	z_1 (Å)	n
B	986.872	2.50134	3.91651	1.70184	0.792464	1.16858	2
A	1025.48	2.52132	3.76974	1.71523	0.799124	1.16424	2
H	449.09	1.24777	2.79878	2.74226	0.854468	2.42661	2

physical significance. This potential essentially differs from that of Ghio for small values of z: while the Ghio potential can be divergent (or may undergo very strong variations) in this domain, ours presents a smooth behavior. The proposed formula (eq 1) lends itself to very good fits of the computed points of the physisorption potential on both sides of the potential well (see below).

Figure 6a shows the fit, using eq 1 with the parameters of Table 1, of the RPBE-DZP DFT points of section IIA1 for H adsorption at the hollow site of an aromatic ring of Gr together with the Ghio potential in the well region. Figure 6b shows our potential and the RPBE-DZP DFT points in the full z range. We have verified that the H-Gr quantum energy levels obtained with this new potential remain the same (up to unsignificant differences) as those obtained by Ghio et al.[28] It may be recalled here that H on Gr chemisorption is possible neither for the hollow site nor for the bridge site[7,8] this is the reason why Figure 6 shows a repulsive behavior for $z < 2$ Å. For the top site the actual potential curve departs from the curve shown in Figure 6 for $z < 2$ Å owing to substrate relaxation and chemisorption.[7–10] Since we consider a flat and rigid surface below this latter aspect is disregarded in the following.

Likewise, the parameters of Table 2 correspond to the fit of O-pyrene results of section IIA2: RPBE-DZP results for the on top and bridge sites (Figure 7a, b) and MP2-ADZ for the hollow site.

The O-Gr potential wells at the different sites, though comparable, show differences in locations and depths as large as 0.3 Å and 20 meV respectively: the surface is more corrugated for O than it is for H. Then in principle, contrary to the H-Gr case, an interaction potential independent of the position on the surface cannot be used. Nevertheless, we can justify such an approximation by two arguments. First, the O to H mass ratio implies that the OH center of mass lies approximately on the O atom. Thus in the incoming stage of the collision treatment, when the O and H atoms approach each other with their center of mass at rest, the O atom does not possess a significant movement parallel to the surface plane. Second, we can consider a potential independent of the position parallel to the surface plane as a "first order approximation" and we can thereafter test the sensitivity of the LH process to the potential (and then to the position) by changing it.

C. OH Potential. The interaction between the O and H atoms is described by a modified Morse potential V_{OH}

$$V_{OH}(r) = D_{OH}[(1 - e^{-u(\beta_{OH}(r-r_{eq})/r_{eq})})^2 - 1] \quad (2)$$

with

$$u(x) = x(1 + b_1x + b_2x^2 + b_3x^3 + b_4x^4) \quad (3)$$

It is usually considered that the characteristics of a physisorbed molecule (equilibrium distance, dissociation energy, normal modes) remain essentially the same as those of the molecule in the gas phase.[39] DZP-RPBE caculations of our own on the O−H potential energy curve in presence of the surface or not indeed confirm this wisdom. In the latter calculations the O atom is fixed at its equilibrium bridged physisorption position and the H atom moves in a plane parallel to the surface and distant from it by 3 Å. Hence, for the dynamics calculations the OH potential is taken to be that of the gas phase. The coefficients (Tables 3, 4) are those of ref 40. The reason for using this accurate potential instead of a simple Morse potential is that the LH probabilities of OH formation are quite sensitive to the asymptotic behavior of V_{OH}.

III. Dynamics

A. Hamiltonian Equations. The Hamiltonian of the system in the laboratory frame is given by the formula

$$H = \frac{\vec{p}_O^{\,2}}{2m_O} + \frac{\vec{p}_H^{\,2}}{2m_H} + V_{Gr-O}(z_O) + V_{Gr-H}(z_H) + V_{OH}(r_{OH}) \quad (4)$$

where the coordinates x and y span the graphite surface and the z coordinate corresponds to the normal to the surface; the $\vec{p}$s and ms are respectively the momenta and masses of the O and H atoms.

Actually, we choose to consider an "in plane motion" parallel to the graphite surface and z_O and z_H perpendicular motions. The overall "in plane" translation motions are separated out and the relative "in plane" motion is thus treated in its center of mass reference frame. As pointed out above, the center of mass is located approximately at the "in plane" position of the O atom.

Let us call $\vec{\rho}$ the position vector of the "in plane" reduced particle associated with the reduced mass $\mu = m_Om_H/(m_O + m_H)$ and let us call $\vec{p}$ the corresponding momentum. The Hamiltonian becomes

$$H = \frac{\vec{p}^{\,2}}{2\mu} + \frac{p_{zO}^{\,2}}{2m_O} + \frac{p_{zH}^{\,2}}{2m_H} + V_{Gr-O}(z_O) + V_{Gr-H}(z_H) + V_{OH}\left(\sqrt{\vec{\rho}^{\,2} + (z_O - z_H)^2}\right) \quad (5)$$

Then, we can study the problem using the "in plane" polar coordinates (ρ, ϕ), leading to

$$H = \frac{1}{2\mu}\left(p_\rho^{\,2} + \frac{l_z^{\,2}}{\rho^2}\right) + \frac{p_{zO}^{\,2}}{2m_O} + \frac{p_{zH}^{\,2}}{2m_H} + V_{Gr-O}(z_O) + V_{Gr-H}(z_H) + V_{OH}\left(\sqrt{\rho^2 + (z_O - z_H)^2}\right) \quad (6)$$

where l_z is the conserved component of the OH angular momentum.

Moreover in our quasi-classical approach, we assume that l_z is quantized by $l_z = m\hbar$ (with $m = 0, \pm1, \pm2,...$). Since the Hamiltonian only depends on l_z^2, we can limit ourselves to positive values of m.

B. Collision and the OH Formation. For different collision energies $E_{coll} = \vec{p}_{in}^{\,2}/2\mu$ and different angular momenta l_z of relative motion of the reacting O and H atoms on the surface we have studied the probability of formation of a (desorbed) OH molecule.

The computations were carried out using a quasi-classical approach. We first determined the quantum ground-state vibration energy of each atom in its physisorption potential and assumed the "classical" atoms to have these energies relative

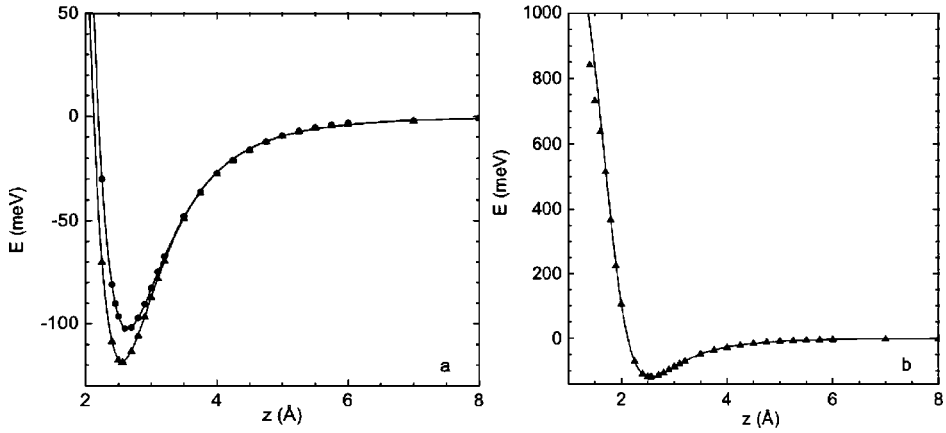

Figure 7. (a) O-pyrene physisorption energies as functions of O-pynene distance. RPBE-DZP bridge site (closed triangles), RPBE-DZP top site (closed circles), fits of eq 1 (full line). (b) Same as Figure 7a for the bridge site and the complete z-range.

TABLE 3: Parameters of the V_{OH} Potential

D (meV)	r_{eq} (Å)	β
4621.19	0.969831	2.227157

TABLE 4: Parameters of the Function u of eq 3

b_1	b_2	b_3	b_4
−0.007791	0.038720	−0.001844	0.001570

to the surface at large interatomic distance. The ground-state vibration energies are: for the hydrogen atom $\epsilon_0 = -35.3$ meV, and for the oxygen atom $\epsilon_0(A) = -96.8$ meV, $\epsilon_0(B) = -111.9$ meV and $\epsilon_0(H) = -107.6$ meV (respectively for the atop, bridge, and hollow sites selected in section 2.2). Moreover, in the initial collision conditions, we assumed (for each atom) a uniform random distribution on the classical phase-space trajectory $(p_z(t), z(t))$ of the atom at the ground-state energy.

A convergence test to the sought probability is implemented into our algorithm. A typical number of 2500 trajectories (for each energy and angular momentum) is necessary to obtain an accuracy of three digits on the formation probability of a (desorbed) OH molecule.

Moreover our program does not contain a fixed time of integration for all trajectories: our algorithm tests at each step (after the first minimum of the interatomic distance) if the system can be assigned as being an outcoming molecule or not. This test combines informations on positions, velocity and energy:

• If the z value z_{cm} of the center of mass of O and H verifies $z_{cm} \geq 15$ Å, with $dz_{cm}/dt \geq 0$ and if the energy of the system in its center of mass frame is negative, a formation of a molecule is validated. If the energy of the system in its center of mass frame is positive, an atomic desorption is validated.

• If $z_{cm} \leq 15$ Å and $r_{OH} \geq 15$ Å with $dr_{OH}/dt \geq 0$ a scattering process is validated.

• Otherwise the integration keeps on, until eventually the upper bound on the integration time (30 ps) is reached.

For each collision energy the number of trajectories that cannot be assigned is recorded (typically less than ten for 2500 trajectories) to verify that the integration time upper bound does not play any role.

C. Results. We have computed the probabilities $P(l_z, E_{coll})$ for the atop, bridge, and hollow potentials V_{O-Gr} of section II.B. The computations have been carried out with a step of 0.2 meV in the range 0.15 meV $\leq E_{coll} \leq$ 4.15 meV most relevant to the ISM and, as a mere indication on how the results extrapolate, with a step of 2 meV in the range 4.15 meV $\leq E_{coll} \leq$ 12 meV. It is recalled that the l_z angular momentum is taken to be quantized: $l_z = m\hbar$, (m = 0, 1, 2, ...).

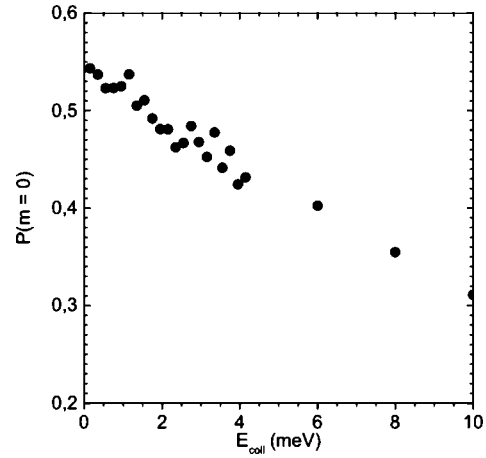

Figure 8. Probability of OH formation via the LH reaction for $l_z = 0$ as a function of the collision energy between the reacting O and H atoms on the surface.

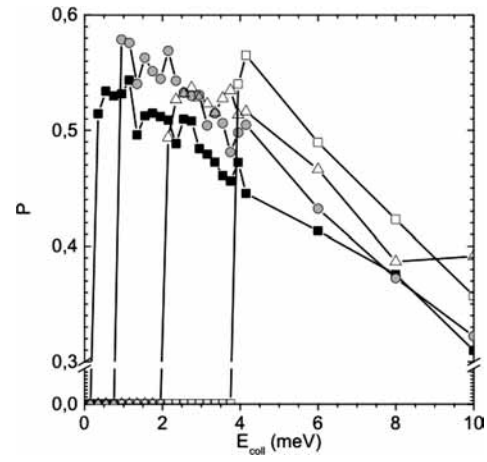

Figure 9. Probability of OH formation via the LH reaction as a function of the collision energy between the reacting O and H atoms on the surface for different values of $l_z = m\hbar$: $m = 1$ closed squares, $m = 2$ circles, $m = 3$ triangles, $m = 4$ open squares.

The results are not very sensitive to the considered V_{O-Gr} potentials: the probabilities differ by about 2%. Accordingly we only present below the results obtained with the Bridge potential.

TABLE 5: Thresholds of $P(l_z, E_{coll})$

l_z	0ħ	1ħ	2ħ	3ħ	4ħ
threshold (meV)	0.0	0.22	0.92	2.13	3.87

1. Probability of OH Formation. First we present the case $l_z = 0$ (Figure 8). At the lowest investigated energies ($E_{coll} \simeq 0.15$ meV), we obtain typically a probability of 54% for the OH formation; the probability decreases with the collision energy. It was not obvious beforehand that such a reaction that involves a heavy atom would occur. It is remarkable that it actually does and in addition with such a large probability.

The computations for different values of the quantized angular momentum l_z (Figure 9) lead to comparable probabilities and evolution with E_{coll} except for a notable feature: there exists an energetic threshold for $l_z \neq 0$. For nonzero l_z values a centrifugal barrier exists that hinders the OH formation at low energy. The thresholds obtained for the first values of $l_z = m\hbar$ are given in Table 5.

2. Quasi-Classical Cross Section. The classical expression of the cross section $\sigma^{Class}(E_{coll})$ is given by the formula

$$\sigma^{Class}(E_{coll}) = \int_{-\infty}^{\infty} P(b, E_{coll})\, db \qquad (7)$$

where b is the projection of the impact parameter onto the surface plane, and $P(b, E_{coll})$ is the reaction probability for a given impact parameter b and a given collision energy E_{coll}. It is related to the l_z angular momentum by the relation $l_z = p_{in}b$ where p_{in} is the initial momentum of the reduced particle in the plane $p_{in} = (2\mu E_{coll})^{1/2}$. We can then rewrite eq 7 as

$$\sigma^{Class}(E_{coll}) = \frac{1}{\sqrt{(2\mu E_{coll})}} \int_{-\infty}^{\infty} P(l_z, E_{coll})\, dl_z \qquad (8)$$

Since the Hamiltonian only depends on l_z^2, the probability law $P(l_z, E_{coll})$ is even in l_z and then

$$\sigma^{Class}(E_{coll}) = \frac{2}{\sqrt{(2\mu E_{coll})}} \int_{0}^{\infty} P(l_z, E_{coll})\, dl_z \qquad (9)$$

Since our treatment considers the quasi-classical rule $l_z = m\hbar$ we can deduce a quantum-like formula for the quasi-classical cross section $\sigma^{QClass}(E_{coll})$

$$\sigma^{QClass}(E_{coll}) = \frac{2\hbar}{\sqrt{(2\mu E_{coll})}} \sum_{m=0}^{\infty} P(m, E_{coll}) \qquad (10)$$

Actually this formula is the true quantum formula if the probabilities $P(m, E_{coll})$ are obtained from quantum mechanics, in our case these probabilities are quasi-classical.

From eq 7 it is seen that $\sigma^{QClass}(E_{coll})$ has the dimension of a length. The LH "cross section" is thus a sort of "efficient length".[27]

Figure 10 displays the $\sigma^{QClass}(E_{coll})$ reaction cross section. In the low energy domain ($E_{coll} \leq 2$ meV) we obtain a typical value of $\sigma^{QClass} \simeq 4.5$ Å. At first sight the structures in the cross section seem strange since we are in a classical context. Actually our treatment is not strictly classical since l_z is quantized. The thresholds of $P(m, E_{coll})$ mentioned in section IIIC1 (Table 5) thereby explain the discontinuities of the cross section. The same phenomenon also appears in the curves presented below for the distributions of the OH excitations.

An important word of caution is in place here. It is well-known that when O(^{3}P) and H(^{2}S) atoms combine, four OH molecular states are formed: $^2\Sigma^-$, $^4\Sigma^-$, $^2\Pi$, $^4\Pi$; the (X)$^2\Pi$ ground-state is the only state considered here. Considering the spin and symmetry degeneracies of the states the statistical weight of the (X)$^2\Pi$ state is 2/9. This statistical weight ought to be taken into account in any practical use of the above results.

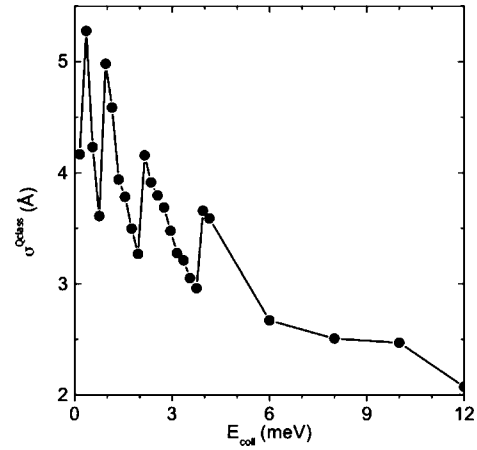

Figure 10. Quasi-classical cross section ("efficient length") of OH formation via the LH reaction as a function of the collision energy between the reacting O and H atoms on the surface.

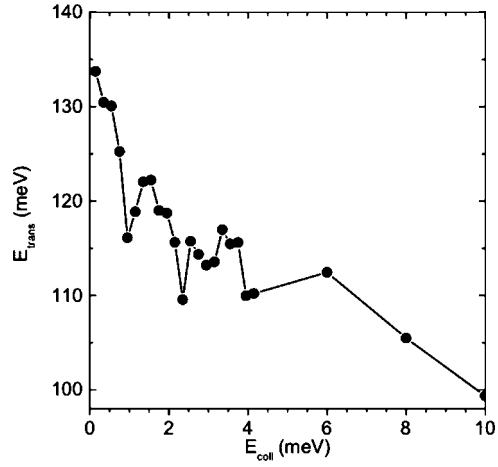

Figure 11. Translation energy of the nascent OH molecule as a function of the collision energy between the reacting O and H atoms on the surface.

3. Distributions of OH Excitations. The OH molecules formed in our LH recombination model are found to be very excited. Such a finding was previously reported in the case of the H−H recombination via the LH mechanism.[26,27] Typically we obtain OH molecules with an internal energy of about 4 eV.

Figure 11 displays the translation energy of the nascent OH molecules E_{trans} as a function of E_{coll}. It is seen that the molecules possess a translation energy of about 125 meV for $E_{coll} \leq 2$ meV.

Figure 12 displays the rotational excitation j of the nascent OH molecules: it shows the average angular momentum normalized to $\hbar$ as a function of E_{coll}. A typical value of $j \simeq 15$ is found in the low energy domain ($E_{coll} \leq 2$ meV).

Figure 13 shows the dependence upon E_{coll} of the OH internal energy measured relative to the OH dissociation limit. In the low collision energy domain $E_{coll} \leq 2$ meV we find internal energies of about −270 meV relative to the O + H dissociation limit. Taking into account the above $j \simeq 15$ value, the latter internal energy may be converted into a vibrational quantum number v; we find $11 \leq v \leq 12$ just below the last bound vibration level.

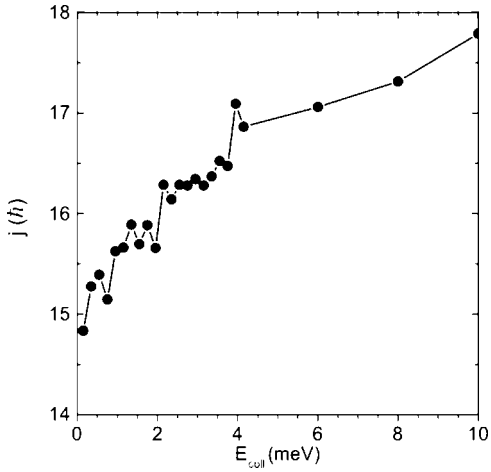

Figure 12. Angular momentum, in units of $\hbar$, of the nascent OH molecule as a function of the collision energy between the reacting O and H atoms on the surface.

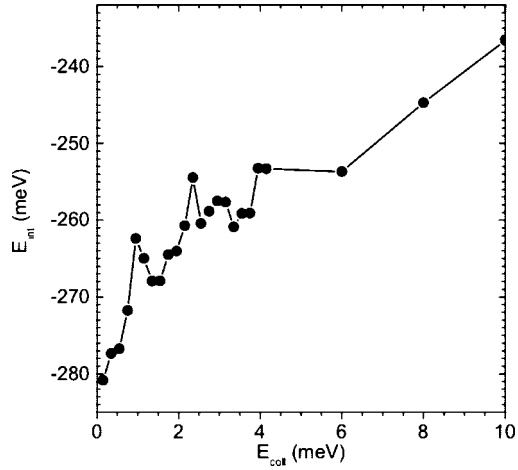

Figure 13. Internal energy, relative to the O + H dissociation limit, of the nascent OH molecule as a function of the collision energy between the reacting O and H atoms on the surface.

D. Discussion. The previous section shows that the main features obtained earlier with the H−H recombination, namely: probabilities and substantial amount of internal energy, remain valid for O−H. In both the H−H and O−H cases the molecule formation reaction is barrier-less and the reaction is highly exothermic: it involves a strongly attractive atom-atom interaction which is 40−100 times greater than the atom−surface physisorption interactions. This produces the molecule in quite high vibration−rotation (v,j) states close to the dissociation limit. This is similar to findings of ref 41 on the ER reaction when the adsorbed atom is weakly bound to the surface.

Nevertheless two important parameters make the O−H and H−H recombination reactions different, namely: O is much heavier than H and the O−Gr physisorption potential is deeper than the H−Gr one. As a consequence it becomes very difficult to imagine that a simple and direct collision between H and O can suffice to extract the O atom from the surface (whereas this direct mechanism, see section I, does exist in the H−H case). In fact our computations show that though this direct mechanism always exists, it is very sensitive to the initial collision conditions and thence it is not very probable. Actually, the "normal" situation for O−H is the creation of a long-lived intermediate OH−Gr complex (complex mechanism, see section I). During the lifetime of this complex, the light atom H undergoes chaotic movements that arise from its numerous collisions with O; it is these repeated O−H collisions that ultimately lead to the extraction of the O atom from the surface.

IV. Summary and Conclusion

With a view to study the O−H recombination on a graphitic surface via the LH mechanism we have first concerned ourselves with the H−Gr and ^{3}O−Gr physisorption characteristics. The reinvestigation of the H−Gr system has led us to propose and use the "well-performing" RPBE-DZP combination in DFT calculations of the physisorption characteristics of the ^{3}O−Gr system. The latter prescription together with MP2-ADZ calculations have enabled us to provide for the first time non empirical information on the ^{3}O−Gr physisorption potentials at the atop, bridge, and hollow sites. These O−Gr physisorption potential wells are 2 to 3 times larger than the H−Gr ones. This has been explained in terms of a charge transfer contribution which, albeit slight, is an order of magnitude larger in the former than in the latter case.

We have also considered O chemisorption and have specifically investigated the triplet spin state case. Our RPBE-DZP calculations provide for the first time the interaction potential along the minimum energy path for ^{3}O adsorption on a graphitic surface. This interaction potential shows two minima: one, at large ^{3}O−Gr distance, is the above-mentioned physisorption well, the other, at shorter distance, corresponds to a "metastable chemisorption" since the well lies above the asymptotic energy level for ^{3}O + Gr at infinite separation. The two wells are separated by an activation barrier of $\approx$ 0.18 eV which make the inner well inaccessible to cold (<2000 K) ^{3}O atoms. H atoms too are prevented from chemisorption by a comparable activation barrier.[7−11] This establishes the soundness of our choice of retaining only physisorption interactions in our investigation of O−H recombination on a graphitic surface via the LH mechanism in the temperature conditions of the ISM.

The model previously used by Morisset et al. [26,27] to treat the H−H recombination on a graphitic surface via the LH mechanism has been extended to study whether O−H recombination is susceptible of occurring in similar conditions. The O to H mass ratio together with the near insensitivity of the mechanism to the V_{O-Gr} physisorption potential validates our approach that does not take into account the corrugation of the surface.

Our quasi-classical calculations show that the reaction indeed takes place. Reaction probabilities and cross sections together with the energy budget of the LH reaction have been determined in a collision energy range of the reacting O and H atoms on the surface (0.15 meV $\leq E_{coll} \leq$ 12 meV) that encompasses typical energies of relevance for the physical chemistry of the ISM. Some basic features obtained earlier with the H−H recombination are unchanged. The OH molecules are formed with a large amount of internal energy and desorb with translational energies of 100−135 meV that are large compared to the mean energies prevailing in the ISM (1−10 meV).

Contrary to what was found in the H−H case the O−H recombination results show that the direct O + H collision followed by OH desorption is an epiphenomenon. The LH mechanism results predominantly from the formation of a long-lived OH−Gr complex in which the H atom repeatedly collides with the O atom before the OH molecule takes off. This opens a possibility of energy exchange between the molecule and the surface during the intermediate complex lifetime which is susceptible of modifying the OH desorption rate and the energy budget of the reaction. Elucidation of this latter issue, which is the subject of ongoing work, is required before one may build

sensible scenarios of X + OH → XOH reactions (especially water, X = H) in the ISM.

Acknowledgment. The authors thank the French program 'Physico-Chimie du Milieu Interstellaire' and programme pluriformations "Carbon matter: from the stars to the laboratory" for financial support. We are grateful to the "Agence Nationale de la Recherche" (ANR) that supports this work in the framework of the IRHONI No. ANR-07-BLAN-0129-2 Project.

References and Notes

(1) Cuppen, H. M.; Herbst, E. *Atrophys. J.* **2007**, *668*, 294.
(2) Miyauchi, N.; Hidakaa, H.; Chigai, T.; Nagaoka, A.; Watanabe, N.; Kouchi, A. *Chem. Phys. Lett.* **2008**, *456*, 27.
(3) Watson, W. D. *Rev. Mod. Phys.* **1976**, *48*, 513.
(4) Ertl, G. *Surf. Sci.* **1994**, *299/300*, 742.
(5) Harris, J.; Kasemo, B. *Surf. Sci.* **1981**, *105*, L281.
(6) Scott, A.; Duley, W. W. *ApJ* **1996**, *472*, L123.
(7) Jeloaica, L.; Sidis, V. *Chem. Phys. Lett.* **1999**, *300*, 157.
(8) Sidis, V. Jeloaica, L. Borisov, A. G. Deutscher, S. A. in Combes, F., Pineau des Forêts, G. Eds.; *Molecular Hydrogen in Space*; Cambridge Contemporary Astrophysics Series, Cambridge University Press: Cambridge, 2000; p 89.
(9) Sha, X.; Jackson, B. *Surf. Sci.* **2002**, *496*, 318.
(10) Ferro, Y.; Marinelli, F.; Allouche, A. *J. Chem. Phys.* **2002**, *116*, 8124.
(11) Zecho, T.; Güttler, A.; Sha, X.; Jackson, B.; Küppers, J. *J. Chem. Phys.* **2002**, *117*, 8486.
(12) Lamoen, D.; Persson, B. N. J. *J. Chem. Phys.* **1998**, *108*, 3332.
(13) Incze, A.; Pasturel, A.; Chatillon, C. *Surf. Sci.* **2003**, *537*, 55.
(14) Sorescu, D. C.; Jordan, K. D.; Avouris, P. *J. Phys. Chem. B* **2001**, *105*, 11227.
(15) Ferro, Y.; Allouche, A.; Marinelli, F.; Brosset, C. *Surf. Sci.* **2004**, *559*, 158.
(16) Jelea, A.; Marinelli, F.; Ferro, Y.; Allouche, A.; Brosset, C. *Carbon* **2004)** , *42*, 3189.
(17) Ferro, Y.; Marinelli, F.; Allouche, A. *Chem. Phys. Lett.* **2003**, *368*, 609.
(18) Perdew, J. P.; Chevary, J. A.; Vosko, S. H.; Jackson, K. A.; Pederson, M. R.; Singh, D. J.; Fiolhais, C. *Phys. Rev. B* **1992**, *46*, 6671.
(19) Svensson, M.; Humbel, S.; Froese, R. D. J.; Matsubara, T.; Sieber, S.; Morokuma, K. *J. Phys. Chem.* **1996**, *100*, 19357.
(20) Humbel, S.; Sieber, S.; Morokuma, K. *J. Chem. Phys.* **1996**, *105*, 1959.
(21) D Becke, A. *Phys. Rev. A* **1988**, *38*, 3098.
(22) Lee, C.; Yang, W.; Parr, R. G. *Phys. Rev. B* **1988**, *37*, 785.
(23) Stephens, P. J.; Devlin, F. J.; Chabalowski, C. F.; Frisch, M. J. *J. Phys. Chem.* **1994**, *98*, 11623.
(24) Goumans, T. P. M.; Uppal, M. A.; Brown, W. A. *Mon. Not. Astron. Soc.* **2008**, *384*, 1158.
(25) Zhao, Y.; Truhlar, D. G. *J. Phys. Chem. A* **2004**, *108*, 6908.
(26) Morisset, S.; Aguillon, F.; Sizun, M.; Sidis, V. *J. Chem. Phys.* **2004**, *121*, 6493.
(27) Morisset, S.; Aguillon, F.; Sizun, M.; Sidis, V. *J. Chem. Phys.* **2005**, *122*, 194702.
(28) Ghio, E.; Mattera, L.; Salvo, C.; Tommasini, F.; Valbusa, U. *J. Chem. Phys.* **1980**, *73*, 556.
(29) Bonfanti, M.; Martinazzo, R.; Tantardini, G. F.; Ponti, A. *J. Phys. Chem. C* **2007**, *111*, 5825.
(30) Tielens, A. G. G. M.; Hagen, W. *Astron. Astrophys.* **1982**, *114*, 245.
(31) Papoular, R. *Mon. Not. R. Astron. Soc.* **2005**, *362*, 489.
(32) Rougeau, N.; Teillet-Billy, D.; Sidis, V. *Chem. Phys. Lett.* **2006**, *431*, 135.
(33) Zhechkov, L.; Heine, T.; Seifert, G. *Int. J. Quantum Chem.* **2006**, *106*, 1375.
(34) Perdew, J. P.; Burke, K.; Ernzerhof, M. *Phys. Rev. Lett.* **1996**, *77*, 3865.
(35) Hammer, B.; Hansen, L. B.; Norskov, J. K. *Phys. Rev. B* **1999**, *59*, 7413.
(36) Amsterdam Density Functional, scientific computing and modelling (SCM), Theoretical Chemistry, Vrije Universiteit, Amsterdam, The Netherlands, http://www.scm.com.
(37) (a) Schmidt, M. W.; Baldridge, K. K.; Boatz, J. A.; Elbert, S. T.; Gordon, M. S.; Jensen, J. H.; Koseki, S.; Matsunaga, N.; Nguyen, K. A.; Su, S. J.; Windus, T. L.; Dupuis, M.; Montgomery, J. A. General Atomic and Molecular Electronic Structure System. *J. Comput. Chem.* **1993**, *14*, 1347. (b) See also: Gordon, M. S.; Schmidt, M. W. Advances in electronic structure theory: GAMESS a decade later In *Theory and Applications of Computational Chemistry, the first forty years*; Dykstra, C. E., Frenking, G., Kim, K. S., Scuseria, G. E. Eds.; Elsevier: Amsterdam, 2005; Chapter *41*, p 1167; http://www.msg.chem.iastate.edu/GAMESS/GAMESS.html.
(38) Makarewicz, J. *J. Chem. Phys.* **2004**, *121*, 8755.
(39) Richardson, N. V.; Sheppard, N. *Vibrational Spectroscopy of Molecules on Surface*; Plenum: NY, 1987).
(40) Martin, J. M. L. *Chem. Phys. Lett.* **1998**, *292*, 411.
(41) Jackson, B.; Lemoine, D. *J. Chem. Phys.* **2001**, *114*, 474.

JP8050966